Med Biol Eng Comput (2015) 53:869–878
DOI 10.1007/s11517-015-1295-6

ORIGINAL ARTICLE

Influence of head mass on temporo-parietal skull impact using finite element modeling

Debasis Sahoo[1] · Caroline Deck[1] · Narayan Yoganandan[2] · Rémy Willinger[1]

Received: 27 January 2014 / Accepted: 1 April 2015 / Published online: 12 April 2015
© International Federation for Medical and Biological Engineering 2015

Abstract The effect of head mass on its biomechanical response during lateral impact to the head is investigated in this computational study. The mass of the head of a state-of-the-art validated finite element head model is altered by ±10 % from the base value of 4.7 kg. Numerical simulations of lateral head impacts for 30 cases (representing 15 human cadaver experiments × 2 mass configurations) are performed using the LS-DYNA solver at different velocities ranging from 2.4 to 6.5 m/s and three impacting conditions representing different stiffness and shapes of the contact/impact surfaces. Results are compared with the original model using the baseline head mass, thus resulting in a total of 45 simulations. Present findings show that the head mass has greater influence for peak interaction forces and the force has a greater dependency on stiffness of contact surface than the shape. Mass variations have also influence on skull strain energy. Regardless of increase/decrease in skull strain energy influenced by head mass variations used in the computational study, the 50 % fracture tolerance limit was unaltered, which was 544 mJ. The present study gives a better understanding of the mechanism of temporo-parietal skull impact.

Keywords Parametric study · Temporo-parietal impact experiments · Peak forces · Finite element model · Skull fracture

✉ Caroline Deck
deck@unistra.fr

[1] Université de Strasbourg ICube, UNISTRA-CNRS, 2 rue Boussingault, 67000 Strasbourg, France

[2] Department of Neurosurgery, Medical College of Wisconsin, 9200 West Wisconsin Avenue, Milwaukee, WI 53226, USA

1 Introduction

The biomechanical response of human head in pedestrian accidents and side-impact motor vehicle crashes leads to temporo-parietal skull fractures in some of the cases [17, 28, 34]. Due to the proximity of interior components of vehicle, the temporo-parietal region of human head often involves in contact during lateral motor vehicle impact [7]. Around 95 % of all diffuse axonal injury (DAI) cases are associated with head contact to the interior surface of the vehicle [29]. Limited studies are reported in the literature in the context of trauma biomechanics of lateral head impact [1, 7, 18, 28, 29]. In contrast to lateral region of head, the frontal impact has been investigated more often, and current regulatory injury criteria adopted worldwide were derived from the integration of the resultant linear acceleration at the center of gravity of head [15]. However, injury criteria derived for frontal impacts may exceed its limits during side impacts, mostly occurred in vehicle crashes [28]. Hence, the applicability of these criteria to temporo-parietal impacts is not promising during side-impact motor vehicle crashes [7]. In-depth study in this field can provide better understanding of skull fracture mechanism and emphasis on the tolerance of the skull to lateral impact.

Quantification of biomechanical tolerance is essential to describe the aspect of head injury in different accident scenarios. There are two widely adapted methods available in the literatures to enumerate the tolerance limit: One is controlled laboratory experiments [33], and the other is numerical computation using mathematical analogue [4–6]. Both the methods have their limitations. There are restrictions and ethical issues to conduct experiments with post-mortem human surrogate (PMHS) specimen. On the other hand, mathematical simulations have the unique ability to

describe the complex geometry, to assess the injury sustained by different parts of the head in various impact conditions and to conduct parametric studies. However, the finite element head model (FEHM) must be validated against appropriate experimental data. Parametric studies are essential when developing new head injury criteria [12, 20].

Variables considered in the parametric analysis include: the input loading characteristics such as the direction and location of the impact loading on the head and impactor mass and energy; material property of the head; and physical properties (e.g., mass and skull thickness) of the head itself. As a first step, Kleiven [13] analyzed the effect of different loading direction in prediction of subdural hematoma. Same loadings were imposed in different directions to a parameterized FEHM and found that the largest brain–skull relative motion occurred with the anterior–posterior and posterior–anterior rotational impulse, and head injury criterion (HIC) was unable to predict the influence of rotational impulse. Horgan and Gilchrist [10] performed parametric studies on the effect of different mesh size and material properties of a three-dimensional (3D) FEHM and found that the short-term shear modulus of the brain tissue had the biggest effect on intracranial frontal pressure and on the von-Mises response. Ruan et al. [19] investigated the biomechanical response of the head to the alteration of impact speed (a measure of input energy), location and impactor mass and found that the higher countercoup pressure occurred from an occipital impact than a frontal impact. Frontal impact simulations were conducted by Ruan and Prasad [20] to evaluate the effect of skull thickness on skull and brain responses. There was an increased protection for skull fracture with the increase in skull thickness. However, regardless of skull thickness, the threshold of skull fracture increased as impact duration decreased and constant HIC curves were determined to be incompetent to assess the risk of skull fracture. Chen and Luo [3] studied on the effect of variation of cranial elasticity modulus, impact duration and contact area of impact to the maximum peak strain of brain by applying triangular pulse loading for simulating impact to a 2D FEHM. The results showed a reduction in strain values in the brain with increase in the above variables. A total of 30 human skulls filled with silicone gel were tested by Sarron et al. [23] to study the injury induced by non-penetrating indentation of the military helmet during ballistic impact. Parametric simulations with a 3D FEHM were conducted, and results showed that the diploe layer played a role in protecting the skull from fracture. Few studies are reported in the literature regarding the parametric influence on lateral impact to the skull and temporo-parietal skull fractures. Zhang et al. [35] conducted free drop tests on PMHS unembalmed heads at different impact velocities and varying contact surface. The results showed that the frontal criterion is not adequate for lateral impact due to the presence of severe rotational head acceleration.

Despite these studies addressing to a certain extent the issue of parametric variables, there is paucity in studies for the influence of physical parameters such as the head mass and size to the real-world accident scenarios. Changes in physical properties of the head not only affect its biomechanics, but also influence loads transmitted via the base of the skull/occipital condyles to the human neck [16, 30]. It is well known that the mass affects the load-carrying capacity and impact response as it is a structural variable. Head mass also varies from specimen to specimen in experimental studies [31]. Regardless of head size influence on intracranial response [12], the effect of head mass on skull fracture and induced peak contact force has not been studied in finite element (FE) head impact simulations. Consequently, the objective of the present study was to determine the role of head mass on the biomechanics of the head and to quantify the tolerance limit for skull fracture in temporo-parietal impact. The objective was achieved parametrically using a validated 3D FEHM.

2 Methods

2.1 The FE head model

The new state-of-the-art FEHM which was enhanced in terms of new constitutive material laws for both brain and skull than the existing FEHM [5, 6] was utilized in the current research for parametric study. The previous FEHM was equivalent to 50th percentile adult human head, and the total mass of head model is 4.7 kg. The main anatomical features include the scalp, the brain, the brainstem and the cerebrospinal fluid (CSF) represented by brick elements and the skull, the face and two membranes (the falx and the tentorium) modeled with shell elements [11]. The physical properties of SUFEHM like circumference, length and breadth are 572, 199 and 154 mm, respectively. The FEHM is composed of 13,208 elements from which 1797 shell elements representing the skull and 5320 brick elements dedicated for the brain. This FEHM was validated against intracranial pressure data from Nahum et al. [14] and Trosseille et al. [25] and the validations were performed by Willinger and Baumgartner [27], Deck et al. [4] under Radioss code and by Deck and Willinger [5, 6] using the LS-DYNA solver. The brain model was enhanced by implementing anisotropy and fiber data (fractional anisotropy and fiber orientation) from medical imaging (diffuse tensor imaging) into new constitutive law [2] and recently validated against local brain motion data from Hardy et al. [8, 9] by Sahoo et al. [21]. The skull model was also improved by using

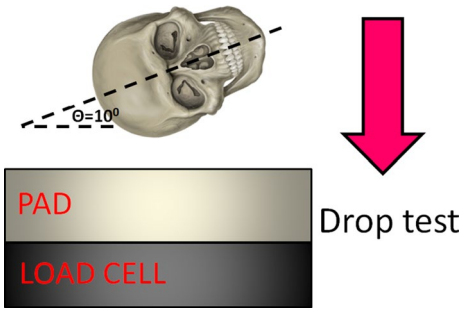

Fig. 1 Test setup for drop test

appropriate composite material model which takes into account the skull fracture by Sahoo et al. [22]. The skull was modeled by a three-layered composite shell representing the inner table, the diploe and the external table of human cranial bone. The material model 55, which was available in the LS-DYNA solver, named as MAT_ENHANCED COMPOSITE_DAMAGE was used to represent the material behavior of skull bones. The material model 55 has three failure criteria for four different types of in-plane damage mechanism based on Tsai and Wu criterion [26]. The new composite skull model was validated not only for maximum forces, but also for lateral impact against actual force–time curves from postmortem human subject (PMHS) impact experiments in the entire time domain at different velocities and for different boundary conditions. This upgraded FEHM was used in this paper to perform parametric studies related to temporo-parietal impact to skull in order to achieve the goals of this investigation.

2.2 Experimental data for the parametric study

The test matrix consists of a total of 86 drop tests from 17 unembalmed PMHS specimens, which were isolated at the level of the occipital condyles. Repeated drop tests were conducted on the same specimen with successively increasing input energies (increasing drop heights) to the specimen until fracture. Three impacting boundary conditions, also termed as targets, were used: flat 40 and 90 durometers (40DF and 90DF) padding (50 mm thickness) and cylindrical 90 durometer (90DC, 50 mm diameter) padding. The abbreviations D, F and C stand for durometer, flat and cylindrical impactor, respectively, in the specimen id. The midsagittal plane of the specimen was aligned at an angle of approximately 10° with respect to the horizontal plane such that the impact was focused onto the left temporo-parietal region as illustrated in Fig. 1. Acceleration and force–time signals were collected using a digital data acquisition system (TDAS Pro, DTS Technologies, Seal Beach, CA) according to the Society of Automotive Engineers, SAE J 211 specifications at a sampling frequency of 12.5 kHz. Signals were processed using SAE Class 1000 filter. Peak resultant forces and center of gravity linear and angular accelerations were obtained for each test. More information about the experiments and the validation of skull FE model in terms of lateral impact and temporo-parietal skull fracture are reported in Sahoo et al. [22].

2.3 Simulation boundary conditions

Using the advanced FEHM with new constitutive material model and side impact—specific experimental data, the sensitivity of biomechanical response to variations in mass was determined in this study. The impact surface was modeled as brick element with MAT 63 CRUSHABLE_FOAM of thickness 50 mm and rested on the top of a rigid platform. More information about the impactor material was reported in Sahoo et al. [22]. The rigid platform was constrained at the bottom to imitate the boundary condition. The CONTACT_AUTOMATIC_SURFACE TO_SURFACE interface was used between the FEHM and impactor with a static friction coefficient of 0.7. The mass of the FEHM was increased and decreased by 10 % to study its effect. The alteration in mass was done by changing the density of different parts of the head model proportionally. The numerical simulations of lateral head impact were performed under LS-DYNA platform for all velocities (ranging from 2.4 to 6.5 m/s) and for three impacting conditions (flat and cylindrical 90D, and flat 40D) for investigating the influence of mass. This resulted in 45 simulations (40DF six velocities, 90DF five velocities and 90DC four velocities, and for ±10 % head mass variations); including 15 simulations with the baseline model which has 4.7 kg head mass. The LS-DYNA solver currently used for the simulation is ls971_d_R5.1.1_win32_p. The resultant contact force curves for each simulation were extracted and compared with the experimental and the simulation results (without variation in mass). Furthermore, the peak strain energy for skull was calculated for each case as a potential parameter to predict skull fracture as described in earlier study [22].

The extracted results from simulations are quantified by calculating the correlation value "*r*" (also known as sample Pearson correlation coefficient) and the percentage difference between the simulation and experimental peak contact forces. For mass variation simulations, the resultant force–time curves are compared with reference mass force interaction plots [22].

3 Results

The resultant contact force–time plots obtained from numerical simulations are plotted for the baseline/reference

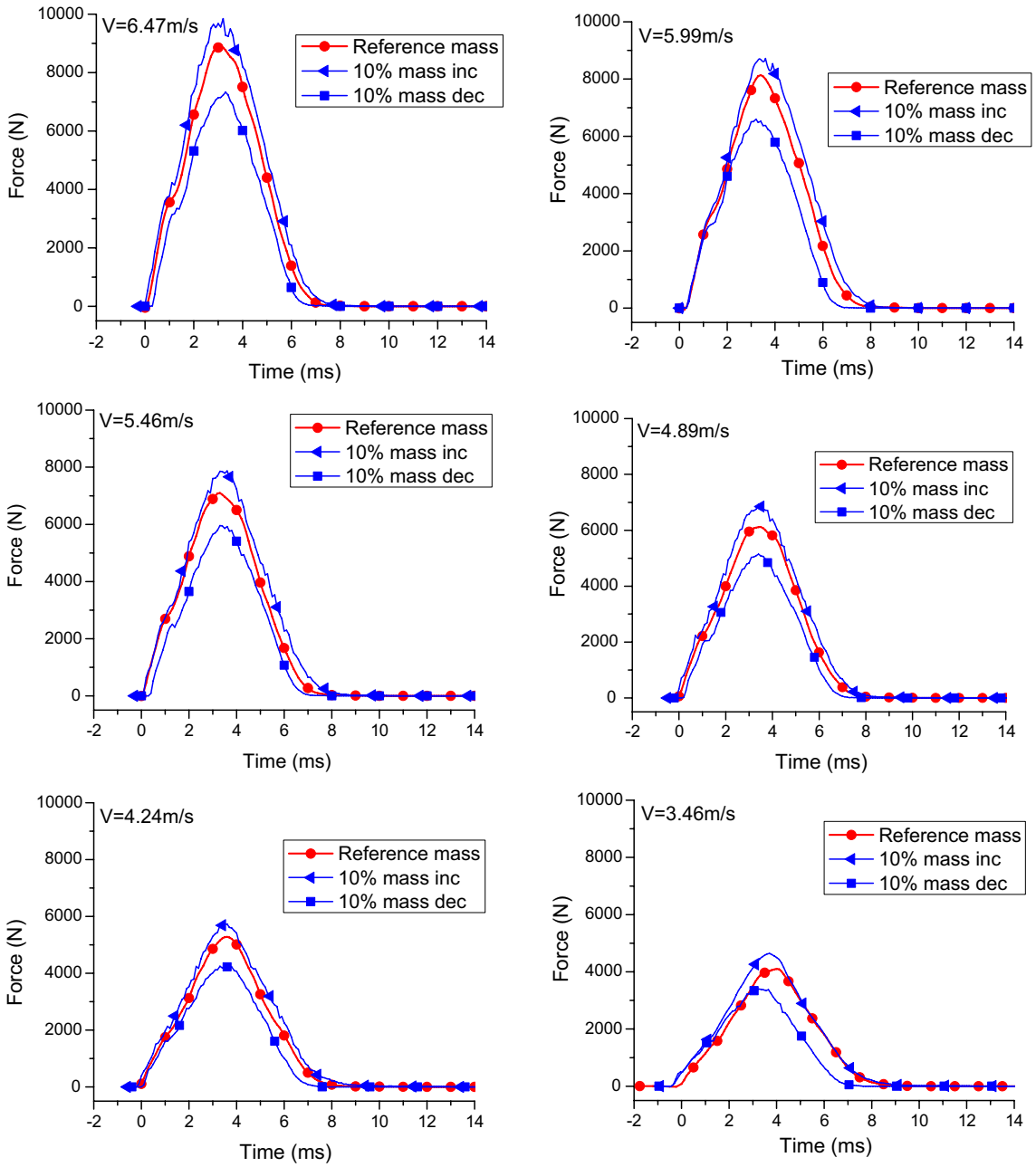

Fig. 2 Comparison of contact force of simulation after increasing or decreasing head mass by 10 % with reference head mass [22] for six different head impact velocities for 40D flat impactor

and ±10 % variations in head mass. The results are filtered at SAE 1000 Hz as per the experiments. Figure 2 shows the comparison of simulation contact forces with the reference contact force [22] for 10 % increase and decrease in head mass for a 40D flat impactor. Twelve simulations were conducted for six different velocities. The velocity ranges from 6.47 to 3.46 m/s in accordance with the experimental data. The peak forces at different velocities are listed in Table 1 for 40D flat impactor. The deviation of peak value of simulation curves from peak of reference contact force curve is calculated for all cases. With the increase in head mass of 10 %, the contact force peak increased by an average of 10.85 %. Similarly, with the decrease in head mass by 10 % the contact force decreased by an average of 17.19 %. The skull strain energies for all the cases were calculated. The comparison of reference skull strain energy [22] with ±10 % mass variation simulation strain energies is shown in Fig. 5a for 40D flat impactor along with the percentage deviation from reference in Fig. 5b. It is observed that with the increase in head mass to 10 %, the skull strain energy

Table 1 Peak forces at different impact velocities for the three impactors

	Peak forces (*N*) for 40D flat impactor					
	$V = 6.47$ m/s	$V = 5.99$ m/s	$V = 5.46$ m/s	$V = 4.89$ m/s	$V = 4.24$ m/s	$V = 3.46$ m/s
Experiment	8695 [7420–9970]	8258 [7150–9420]	7635 [6810–8460]	6630 [6010–7250]	5650 [5000–6300]	3985 [3330–4640]
Simulation Ref. [22]	8878	8140	7094	6117	5279	4100
+10 % mass	9850	8823	7868	6932	5725	4637
−10 % mass	7436	6595	5959	5148	4283	3395

	Peak forces (*N*) for 90D flat impactor				
	$V = 5.46$ m/s	$V = 4.89$ m/s	$V = 4.24$ m/s	$V = 3.46$ m/s	$V = 2.44$ m/s
Experiment	9765 [6830–12,700]	9215 [7230–11,200]	8430 [6760–10,100]	6890 [5670–8110]	4545 [3930–5160]
Simulation Ref. [22]	9820	8748	7557	6241	4240
+10 % mass	10,675	9484	8061	6569	4686
−10 % mass	8412	7561	6578	5397	3973

	Peak forces (*N*) for 90D cylindrical impactor			
	$V = 4.89$ m/s	$V = 4.24$ m/s	$V = 3.46$ m/s	$V = 2.44$ m/s
Experiment	7280 [5060–9500]	7110 [6530–7690]	6315 [5240–7390]	4050 [3620–4480]
Simulation Ref. [22]	7158	6836	5806	3866
+10 % mass	7676	7114	6386	3951
−10 % mass	6172	6214	5179	3578

Min–Max = corridors of experiment

increased by 14 % (average of six cases) and with decrease in head mass to 10 % the skull strain energy decreased by 20.66 % (average of six cases).

Figure 3 shows the comparison of simulation contact force with upper and lower corridors for 10 % increase and decrease in head mass, respectively, for 90D flat impactor. Ten simulations were conducted for five different velocities. The velocity ranges from 2.44 to 5.46 m/s in accordance with the experimental data. The peak forces at different velocities are listed in Table 1 for 90D flat impactor. With the increase in head mass of 10 %, the contact force peak increased by an average of 7.91 %. Similarly, with the decrease in head mass by 10 % the contact force decreased by an average of 12.134 %. The skull strain energies for all the cases were calculated. The comparison of reference skull strain energy [22] with ±10 % mass variation simulation strain energies is shown in Fig. 5c for 90D flat impactor along with the percentage deviation from reference in Fig. 5d. It is observed that with the increase in head mass to 10 %, the skull strain energy increased by 10.12 % (average of five cases) and with decrease in head mass to 10 % the skull strain energy decreased by 17.59 % (average of five cases).

Figure 4 shows the comparison of simulation contact force with upper and lower corridors for 10 % increase and decrease in head mass, respectively, for 90D cylindrical impactor. A total of eight simulations were conducted for four different velocities. The velocity ranges from 2.44 to 4.89 m/s in accordance with the experimental data. The peak forces at different velocities are listed in Table 1 for 90D cylindrical impactor. With the increase in head mass of 10 %, the contact force peak increased by an average of 5.87 %. Similarly, with the decrease in head mass by 10 % the contact force decreased by an average of 10.28 %. The skull strain energies for all the cases were calculated. The comparison of reference skull strain energy [22] with ±10 % mass variation simulation strain energies is shown in Fig. 5e for 90D cylindrical impactor along with the percentage deviation from reference in Fig. 5f. It is observed that with the increase in head mass to 10 %, the skull strain energy increased by 10.31 % (average of four cases) and with decrease in head mass to 10 % the skull strain energy decreased by 20.9 % (average of four cases).

4 Discussion

As stated in the introductory paragraphs of the paper, it is well known that the biomechanical response of the human skull depends on the loading direction and, in particular, lateral impact is different from frontal impact, and furthermore, the applicability of frontal impact criterion for side impact of skull is not fully established. Due to the proximity of interior components of vehicle, the temporo-parietal

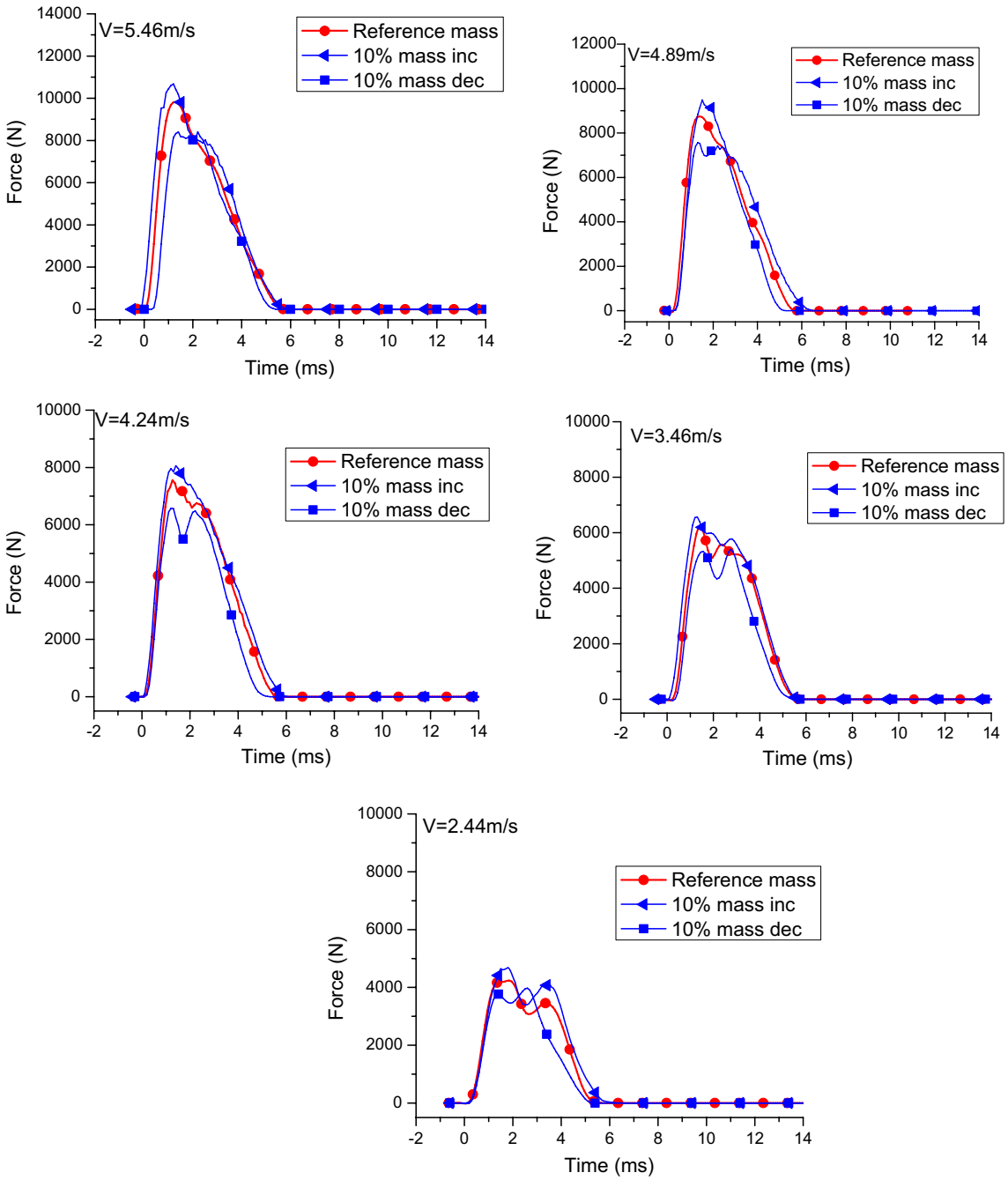

Fig. 3 Comparison of contact force of simulation after increasing or decreasing head mass by 10 % with reference head mass [22] for six different head impact velocities for 90D flat impactor

region of human head often involves in contact during lateral motor vehicle impact [7]. Around 95 % of all DAI cases are associated with head contact to the interior surface of the vehicle [29]. As the human head mass is variable and is one of the physical variables that may influence the output of stress analysis, in the present research, the influence of alterations in the head mass at the instant of temporo-parietal impact to various biomechanical responses was investigated [31]. This was achieved by using a validated FE model with experimental data from human cadaver heads at the temporo-parietal site and conducting parametric studies [22]. Head mass was varied from high to low, representing ±10 % change from the standard head mass used in the validation process. The velocity of impacts varied from 2.4 to 6.5 m/s as in the experiments conducted with PMHS. The impact speed was increased

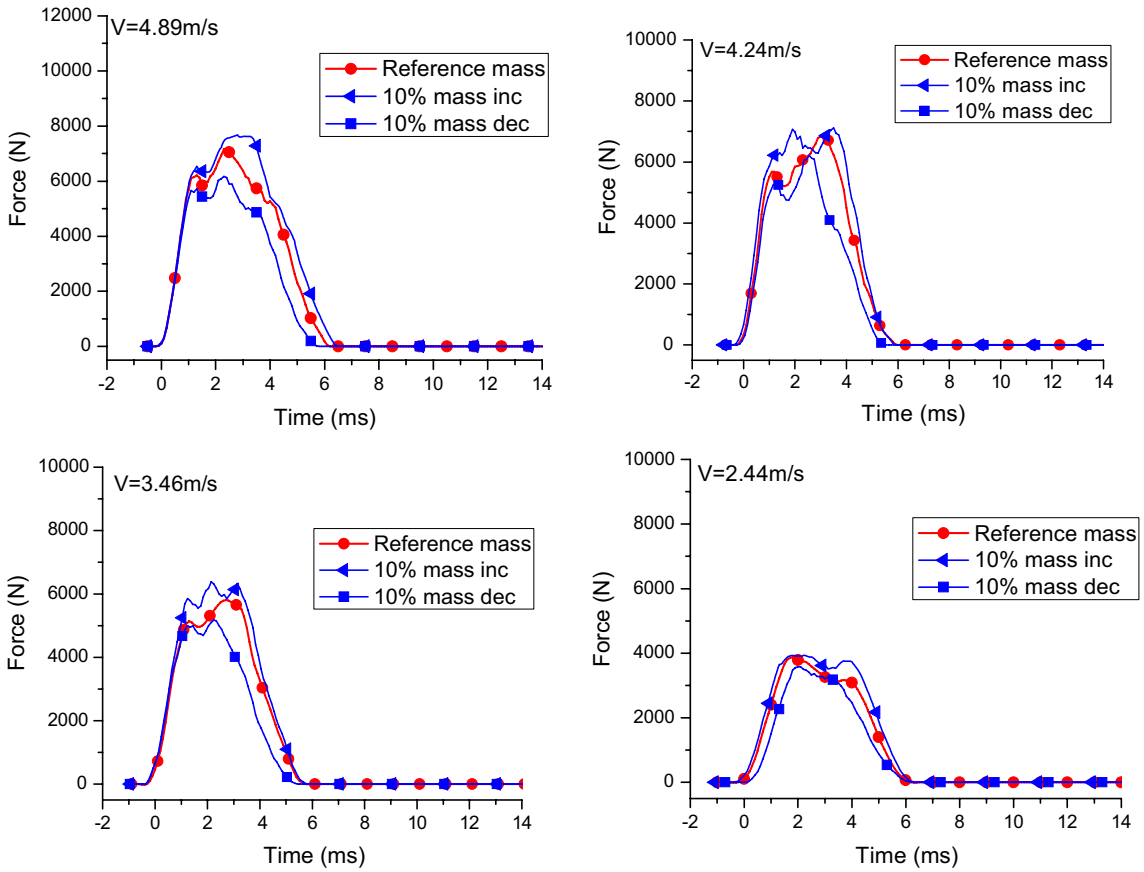

Fig. 4 Comparison of contact force of simulation after increasing or decreasing head mass by 10 % with reference head mass [22] for six different head impact velocities for 90D cylindrical impactor

gradually until fracture occurred to the skull with a drop test technique for each specimen. As it was observed that there were occurrences of fracture for the test batch at this range of velocity with different impactors, it was believed that there will be fracture at higher velocities [22, 28]. The aim was to get the fracture limit during the experiments as well as in the numerical simulations.

As shown in the "Results" section, the influence of the low and high magnitudes of head mass was analyzed with three impacting boundary conditions, flat 40 and 90 durometers and cylindrical 90 durometer and two types of surfaces, flat and cylindrical. In addition, the study used velocities ranging from 2.4 to 6.5 m/s, used in the PMHS experiments to analyze the effect of velocity on head mass variations in terms of examining the peak force, variation of the force–time responses and strain energy density variables. It should be noted that human cadaver experiments did not encompass all velocities for all impacting boundary conditions [28]. However, as shown in Figs. 2, 3 and 4, the role of the head mass was such that higher head mass results in greater peak forces than the lower head mass, an expected result. For a given stiffness of the impacting surface, the lower durometer was responsible for the decreased forces, and this was true for all velocities. However, for the same durometer condition, peak forces were lower with the cylindrical than the flat impacting surface, and this may be attributable to the reduced contact area of the former boundary condition. However, the percentage change in the peak forces was such that the lower durometer accounted for greater changes than the higher durometer (Table 1; 8.4–13.3 vs. 5.3–10.5 % for the 40D and 90D flat surfaces for the high mass; −15.8 to −18.8 vs. −6.3 to −14.3 % for the 40D and 90D flat surfaces for the low mass); at the same 90 durometer level, they were not considerably different (5.3–10.5 vs. 2.2–10.0 % for the flat and cylindrical surfaces for the high mass; −6.3 to −14.3 vs. −7.4 to −13.8 % for the flat and cylindrical surfaces for the low mass). These findings suggest that the peak force magnitude is more dependent on velocity and stiffness than the shape of the impacting surface, although the local distribution of the impact energy and skull deformation fields might be different. This phenomenon was found to be true for the range in mass considered in the present study. These findings quantify the role of mass on the development

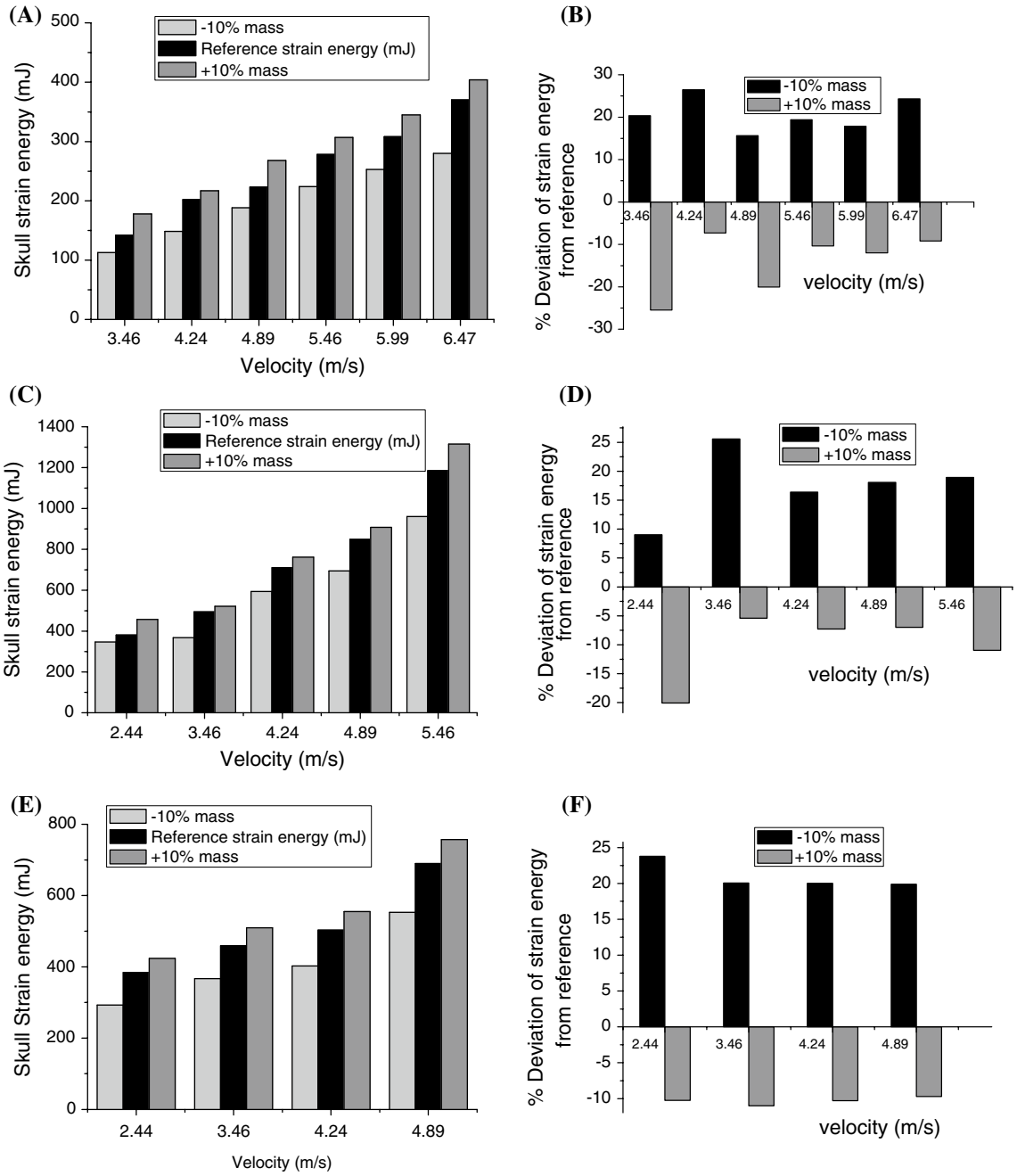

Fig. 5 **a** Skull strain energy comparison. **b** Percentage of deviation in skull energy from reference comparison with ±10 % mass variations for 40D flat impactor. **c** Skull strain energy comparison. **d** Percentage of deviation in skull energy from reference comparison with ±10 % mass variations for 90D flat impactor. **e** Skull strain energy comparison. **f** Percentage of deviation in skull energy from reference comparison with ±10 % mass variations for 90D cylindrical impactor

of maximum force at different levels of external energy imparted to the human head.

Another parameter investigated was the skull strain energy. This secondary variable showed that regardless of the type of impacting surface or the durometer, the average change across all velocities was essentially invariant for the high (10.1–14 % for the 40D and 90D flat and 90D cylindrical surface) and low (17.59–20.9 % for the 40D and 90D flat and 90D cylindrical surface) mass heads. However, the change was more pronounced for the lower mass. This may be due to the limitation of the study which did not take into account factors such as the change in size of the head which may be present concomitant with the altered head mass. The uniform scaling of mass of all head

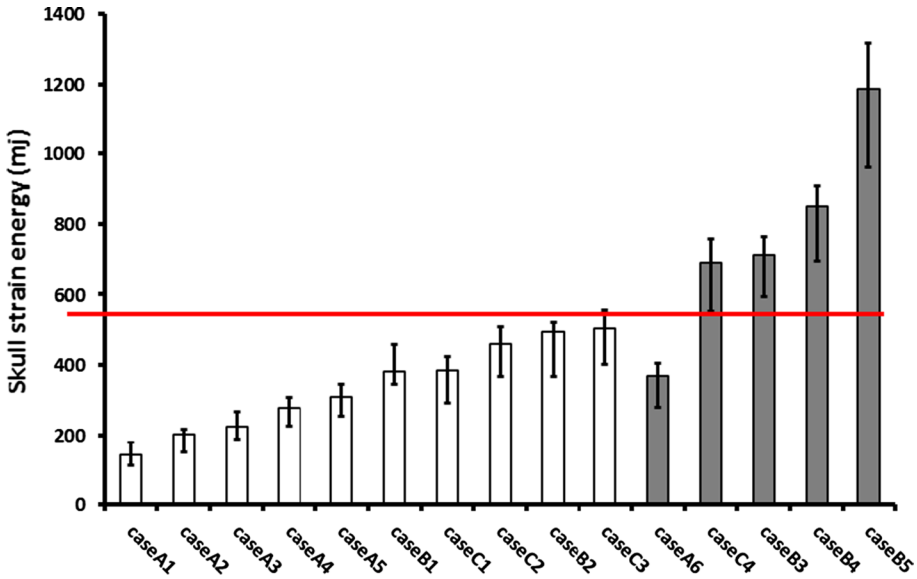

Fig. 6 Skull strain energy for each case along with strain energy at ±10 % mass variation (shown by *black vertical lines* on each column). The *white columns* are for cases without fracture, and *gray columns* are for with fracture. The *solid horizontal line* represents the 50 % risk of skull fracture (544 mJ) [22]

components may be little different than the real mass distribution in smaller and larger heads which may influence the metrics in local loadings. The thickness of skull is another variable which may influence the magnitude of this secondary variable. Also, the shape of the head can vary with head mass, and in order to examine these factors, a multipronged approach may be necessary. From this perspective, while acknowledging the limitation and the need to conduct additional experimental studies to obtain suitable geometric data, it can be concluded that the force–time histories and peak forces are influenced by the mass of the head. The variation of skull strain energies for all the cases is superimposed into the strain energy data for the reference mass [22] as shown in Fig. 6. All the simulations are labeled as Case A, Case B and Case C as in Sahoo et al. [22] and are representing SUFEHM impact simulations on 40D flat, 90D flat and 90D cylindrical padding, respectively. The white columns represent the cases with no skull fracture, and the gray columns represent the cases with fracture. The black line on each column represents the increase or decrease in strain energy with 10 % mass of head increase and decrease, respectively. For most of the cases, mass variation does not affect the fracture criterion as shown by red line in Fig. 6. In all the cases, the criterion for 50 % risk of skull fracture is not affected by parameter (head mass) variation, which demonstrates the robustness of the criterion. The use of FE model and FE simulations are well accepted nowadays in the field of head trauma biomechanics. This current FEHM and criteria for 50 % risk of skull fracture can be used to evaluate and optimize the head protective systems.

The following limitations are applicable to the present study. It is known that head injuries can be comprised of bone fractures and/or brain injuries in real world. The current study was focused only on the former type of injury. It is well known that severe brain traumas such as diffuse axonal injuries are accompanied by head contact loading in motor vehicle environments [24, 29, 32]. It is first important to know the behavior of the skull and its force development/attenuation, and brain injury simulation model should incorporate the skull deformation and interaction with the contained brain tissue for a better understanding of head injuries. The present study has demonstrated the effects of head mass on skull loading, and the next step would be to incorporate these effects into brain injury models.

5 Conclusions

The influence of variations in the head mass during lateral impacts to the head was investigated in this study using a parametric approach and FE modeling. Different impacting boundaries and durometers and velocities were used in the analysis of peak forces, force–time responses and skull strain energies for all cases. Head mass was changed from a high to a low value (increase and decrease by 10 %) compared to the original magnitude used in the FE model. Results indicated that the mass of the head has a greater influence on the development of impact force than the strain energy. Further, the changes in the peak forces were more affected by the changes in the durometer than the shape of the impacting boundary. The overriding influence of the stiffness of the contacting surface may be a factor to consider whether peak forces are to be reduced in impact environments although the shape of the surface at a given durometer level reduces the development of the maximum force on the lateral side of the human head. The influence of mass variation to the skull strain energy was

also studied. Regardless of increase/decrease in skull strain energy influenced by head mass variation, the 50 % fracture tolerance limit was unaltered, which was 544 mJ. The present study gives a better insight into the mechanism of temporo-parietal skull impact and improves the confidence to do further simulation of real-world accident cases.

Acknowledgments The authors acknowledge the ANR-12-EMMA-0026-0 (SUFEHM-13) and VA medical research for their research support to this work.

References

1. Allsop DL, Perl TR, Warner CY (1991) Force/deflection and fracture characteristics of the temporo-parietal region of the human head. Society of Automotive Engineering. SAE Paper No. 912907
2. Chatelin S, Deck C, Willinger R (2012) An anisotropic viscous hyperelastic constitutive law for brain material finite element modeling. J Biorheol. 1–12, ISSN 1867-0466. doi:10.1007/s12573-012-0055-6
3. Chen H, Luo Y (2010) Parametric study of closed head injuries. Adv Theor Appl Mech 3(7):339–347
4. Deck C, Nicolle S,Willinger R (2004) Human head FE modelling: improvement of skull geometry and brain constitutive laws. In: Proceedings on the IRCOBI conference, Graz, pp 79–92
5. Deck C, Willinger R (2008) Improved head injury criteria based on head FE model. Int J Crashworthiness 13(6):667–678
6. Deck C, Willinger R (2008b) Head injury prediction tool for predictive systems optimization. In: 7th European LS-DYNA conference
7. Gennarelli T, Pintar F, Yoganandan N, Beuse N, Morgan R (2002) Head injuries to nearside occupants in lateral impacts: epidemiological and full-scale crash test analyses. In: Proceedings of the IRCOBI. Munich, Germany, pp 223–233
8. Hardy WN, Foster CD, Mason MJ, Yang KH, King AI, Tashman S (2001) Investigation of head injury mechanisms using neutral density technology and high-speed biplanar X-ray. Stapp Car Crash J 45:337–368
9. Hardy WN, Mason MJ, Foster CD, Shah CS, Kopacz JM, Yang KH, King AI, Bishop J, Bey M, Anderst W, Tashman S (2007) A study of the response of the human cadaver head to impact. Stapp Car Crash J 51:17–80
10. Horgan TJ, Gilchrist MD (2003) The creation of three-dimensional finite element models for simulating head impact biomechanics. Int J Crashworthiness 8(4):353–366
11. Kang HS, Willinger R, Diaw BM, Chinn B (1997) Validation of a 3D human head model and replication of head impact in motorcycle accident by finite element modeling. In: Proceeding of 41th Stapp Car Crash Conference, Society of Automotive Engineers, Lake Buena Vista, USA, pp 329–338
12. Kleiven S, von Holst H (2002) Consequences of head size following trauma to the human head. J Biomech 35(2):153–160
13. Kleiven S (2003) Influence of impact direction to the human head in prediction of subdural hematoma. J Neurotrauma 20(4):365–379
14. Nahum A, Smith R, Ward C (1977) Intracranial pressure dynamics during head impact. In: Proceeding of 21st Stapp Car Crash Conference, SAE Paper No. 770922
15. NHTSA (2002) Code of federal regulations, Title 49, Part 571. National highway traffic safety administration, federal motor vehicle safety standards, Washington, DC
16. Pintar FA, Yoganandan N, Baisden J (2005) Characterizing occipital condyle loads under high-speed head rotation. Stapp Car Crash J 49:33–47
17. Pintar FA, Maiman DJ, Yoganandan N (2007) Injury patterns in side pole crashes. Annu Proc Assoc Adv Automot Med 51:419–433
18. Raymond D, Van Ee C, Crawford G, Bir C (2009) Tolerance of the skull to blunt ballistic temporo-parietal impact. J Biomech 42(15):2479–2485
19. Ruan JS, Khalil T, King AI (1993) Finite element modeling of direct head impact. In: Proceedings of 37th Stapp Car Crash Conference, SAE Paper No. 933114, San Antonio, TX
20. Ruan J, Prasad P (2001) The effects of skull thickness variations on human head dynamic impact responses. Stapp Car Crash J 45:395–414
21. Sahoo D, Deck C, Willinger R (2013) Development and validation of an advanced anisotropic visco-hyperelastic human brain FE model. JMBBM. doi:10.1016/j.jmbbm.2013.08.022
22. Sahoo D, Deck C, Yoganandan N, Willinger R (2013) Anisotropic composite human skull model and skull fracture validation against temporo-parietal skull fracture. JMBBM 28:340–353
23. Sarron JC, Caillou JP, Da Cunha J, Allain JC, Tramecon A (2000) Consequences of nonpenetrating projectile impact on a protected head: study of rear effects of protections. J Trauma 49(5):923–929
24. Tagliaferri F, Compagnone C, Yoganandan N, Gennarelli TA (2009) Traumatic brain injury after frontal crashes: relationship with body mass index. J Trauma 66(3):727–729
25. Trosseille X, Tarriere C, Lavaste F, Guillon F, Domont A (1992) Development of a F.E.M. of the human head according to a specific test protocol. In: Proceedings of 36th Stapp Car Crash Conference, SAE Paper No. 922527
26. Tsai SW, Wu EM (1971) A general theory of strength for anisotropic materials. J Compos Mater 5:58–80
27. Willinger R, Baumgartner D (2003) Human head tolerance limits to specific injury mechanisms. Int J Crashworthiness 8(6):605–617
28. Yoganandan N, Pintar FA (2004) Biomechanics of temporo-parietal fracture. Clin Biomech 19:225–239
29. Yoganandan N, Gennarelli TA, Zhang J, Pintar FA, Takhounts E, Ridella SA (2009) Association of contact loading in diffuse axonal injuries from motor vehicle crashes. J Trauma 66:309–315
30. Yoganandan N, Maiman DJ, Guan Y, Pintar F (2009) Importance of physical properties of the human head on head–neck injury metrics. Traffic Injury Prev 10:488–496
31. Yoganandan N, Pintar FA, Zhang J, Baisden JL (2009) Physical properties of the human head: mass, center of gravity and moment of inertia. J Biomech 42:1177–1192
32. Yoganandan N, Baisden JL, Maiman DJ, Gennarelli TA, Guan Y, Pintar FA, Laud P, Ridella SA (2010) Severe-to-fatal head injuries in motor vehicle impacts. Accid Anal Prev 42(4):1370–1378
33. Yoganandan N, Stemper BD, Pintar FA, Maiman DJ (2011) Use of postmortem human subjects to describe injury responses and tolerances. Clin Anat 24:282–293
34. Zhang J, Yoganandan N, Pintar FA, Gennarelli TA (2006) Brain strains in vehicle impact tests. Annu Proc Assoc Adv Automot Med 50:1–12
35. Zhang J, Yoganandan N, Pintar FA (2009) Dynamic biomechanics of the human head in lateral impacts. Annu Proc Assoc Adv Automot Med 53:249–256